Eur. Phys. J. A (2024) 60:114
https://doi.org/10.1140/epja/s10050-024-01335-1

THE EUROPEAN PHYSICAL JOURNAL A

Regular Article - Theoretical Physics

An NJL model analysis of a magnetised nonextensive QCD medium

Chowdhury Aminul Islam[1,2,a]

[1] Institut für Theoretische Physik, Johann Wolfgang Goethe-Universität, Max-von-Laue-Str. 1, D-60438 Frankfurt am Main, Germany
[2] School of Nuclear Science and Technology, University of Chinese Academy of Sciences, 100049 Beijing, China

Received: 16 December 2023 / Accepted: 9 May 2024

Communicated by Tamas Biro

Abstract We investigate the effect of a background magnetic field when applied to a nonextensive QCD medium in a $2+1$ flavour Nambu— Jona-Lasinio model. The effect of a constant as well as an eB-dependent coupling is considered. For the constant coupling, the well-known magnetic catalysis effect is observed with reduced strength in both the condensates and the transition temperatures compared to the standard extensive medium. In the case of a field-dependent coupling, we observe a competition between the nonextensive parameter, q and eB. With sufficiently high q-values, the phenomenon of inverse magnetic catalysis —, a well-known trait in effective models featuring eB-dependent coupling, appears to be eliminated within the range of magnetic fields examined in our present study.

1 Introduction

The creation of a strong magnetic field in heavy-ion collisions (HIC) is now an established fact. Its strength in non-central collisions can be huge as compared to any known terrestrial or extraterrestrial magnetic field-generating phenomenon. Depending on the collisional energy the strength of the magnetic field can vary between $\sim 1-15\, m_\pi^2$ from Relativistic Heavy Ion Collider (RHIC) to Large Hadron Collider (LHC) [1].

From the later half of the first decade in this century, the effect of the magnetic field on the properties of the QCD medium have been explored extensively using both theoretical and experimental techniques [2,3]. Numerous novel phenomena have been proposed and studied in that context, some of the most studied ones are magnetic catalysis (MC) [4], inverse magnetic catalysis (IMC) [5,6], chiral magnetic effect [7], chiral separation effect [8,9] etc. Those interested can delve into an engaging review article that examines a spectrum of potential novel non-dissipative phenomena in the presence of magnetic fields and beyond [10].

On the other hand, in the pursuit of understanding the data from HIC experiments both in RHIC and LHC one statistical distribution, recently, has gained a lot of attention [11–15]. This is widely known as the Tsallis distribution after Constantino Tsallis who in his famous paper [16] investigated the possibility of a nonextensive form of entropy involving a parameter q. The extensive nature of the entropy is obtained back in the limit $q \to 1$. As compared to the exponentials in traditional Boltzmann-Gibbs (BG) extensive statistics, the nonextensive statistics lead to power laws. Its application is found in almost every branch of physics [17].

Its applicability to describe the fireball created in HICs stems from the following facts. The fireball is finite, rapidly evolving in nature and also experiences strong intrinsic fluctuations and long-range correlations. These characteristics render the system non-uniform and global equilibrium cannot be established. As a consequence, some quantities develop power law tailed behaviour and the nonextensive statistics becomes applicable.

There are multiple versions of the Tsallis distribution available in the literature [16,18–20]. Theoretical issues concerning the thermodynamic consistency while implementing Tsallis distribution in the case of relativistic high energy distribution [21,22] have been clarified in Refs. [23,24]. A recent review on the topic concerning nuclear and particle physics can be found in Ref. [25].

There have also been multiple developments in applying nonextensive statistics in QCD-based effective model describing both the hadronic and quark degrees of freedoms [26–31]. These studies, among other things, discussed scalar and vector meson fields, properties of π and σ mesons, chiral symmetry restoration, effect of background gauge field

[a] e-mail: chowdhury.aminulislam@gmail.com, chowdhury@physik.uni-frankfurt.de (corresponding author)

Published online: 24 May 2024

(Polyakov loop field), characteristics of magnetisation, thermodynamic properties of QCD medium etc.

Existing literatures on utilising the effective models for a nonextensive QCD medium do not incorporate the background magnetic field [27–29,31]. On the other hand, there have been ample efforts to understand the effects of MC, IMC and magnetic properties like magnetisation, magnetic susceptibility, etc., of the QCD medium in different effective models [32–39], albeit using extensive statistics. Thus, there is currently a gap in the existing literature regarding effective models for a nonextensive QCD medium that is also magnetized.

Keeping this in mind, in the present work, we shall present a nonextensive version of the Nambu— Jona-Lasinio (NJL) model describing a magnetised QCD medium. Specifically, chiral symmetry restoration while intertwined with nonextensiveness and magnetic field will occupy the central stage of our investigation. Such a study, besides addressing the existing theoretical gap, could have relevance for understanding magnetized QCD media with strong intrinsic fluctuations, long-range interactions, etc., potentially encountered in heavy-ion collision experiments. We start our investigation for the nonextensive statistics with a zero magnetic field (eB) for $2+1$ flavours to put things into perspective. Then we move to the case of nonzero strength of eB. To gauge the effect of the nonextensive statistics we execute the analysis for BG statistics in parallel. We perform the analysis in presence of eB considering different possible scenarios.

First, we check results for the standard NJL model where the coupling constant is independent of eB. Our result shows that at a specific magnetic field strength, the impact of increasing q resembles that of the zero magnetic field case. It leads to a decreasing trend in both the condensates and the transition temperatures. We find out that the model produces the MC effect in Tsallis statistics as well. However, it results in reduced strength in both the condensates and the transition temperatures compared to the BG statistics.

Then, we take our analysis to the case of a magnetic field dependent coupling constant. We choose to work with a coupling constant whose dependence on eB has been determined by fitting to the available lattice QCD (LQCD) data, which produces the IMC effect [33]. We discover that there is a competition between the two parameters q and eB. This is one of the most important findings of the present analysis. Depending on their strengths the observed IMC effect in BG statistics can be eliminated.

Our findings also suggest that with eB-dependent G_S the trend of the transition temperature is non-monotonic. For smaller values of q, such as $q = 1.05$, it remains constant initially and then starts decreasing with increasing magnetic field. With further increment in q, it exhibits a non-monotonic trend as a function of eB: initially it increases and then starts falling. To render the present analysis complete, we also explore the basic form of the coupling constant inspired by Ref. [40], in which the strong coupling α_s decreases with increasing eB and put it in the appendix.

The remainder of the manuscript is organised as follows: First, we provide a brief review on the formalism for $2+1$ flavour NJL model in Sect. 2. We start with the standard NJL model in BG statistics in Sect. 2.1 and then extend it to the nonextensive statistics in Sect. 2.2. In Sect. 3, we thoroughly discuss our findings and compare them with the known results for detailed analysis and comparison. Finally, in Sect. 4, we summarise the conclusion.

2 Formalism

2.1 Extensive statistics

In this section, we briefly revisit the NJL model in the standard extensive scenario. The $2+1$ flavour NJL Lagrangian in presence of a magnetic field can be written as [32,35,41–47],

$$\mathcal{L}^B_{\rm NJL} = \bar{\psi}(i\not{D} - m_0)\psi + \mathcal{L}_1 + \mathcal{L}_2 - \frac{1}{4}F^{\mu\nu}F_{\mu\nu}, \tag{1}$$

where $m_0 = \text{diag}(m_u, m_d, m_s)$ with $m_u = m_d$; $\not{D} = \gamma_\mu D^\mu$ with $D^\mu = \partial^\mu - iqA^\mu$ and q being the electric charge ($q_u = 2/3e, q_d = -1/3e$ and $q_s = -1/3e$); e is the charge of a proton, $F^{\mu\nu} = \partial^\mu A^\nu - \partial^\nu A^\mu$ is the field strength tensor and A^μ being the electromagnetic gauge field. The Lagrangians $\mathcal{L}_1$ and $\mathcal{L}_2$ are [48–50]

$$\mathcal{L}_1 = \frac{G_S}{2}\sum_{a=0}^{8}[(\bar{\psi}\lambda_a\psi)^2 + (\bar{\psi}i\gamma_5\lambda_a\psi)^2] \text{ and} \tag{2}$$

$$\mathcal{L}_2 = -G_D\{\det[\bar{\psi}(1+\gamma_5)\psi] + \det[\bar{\psi}(1-\gamma_5)\psi]\}. \tag{3}$$

The Lagrangian $\mathcal{L}_1$ is usually called the symmetric Lagrangian as it respects the full global symmetry of QCD, $SU(3)_V \times SU(3)_A \times U(1)_V \times U(1)_A$. On the other hand, $\mathcal{L}_2$ breaks the $U(1)_A$ symmetry and is responsible for the axial anomaly found in QCD. It is known as the 't Hooft determinant term or simply the determinant term.

Before obtaining the thermodynamic potential, one must note a few important things. Because of the presence of the magnetic field there are some important modifications in the calculation. First, the dispersion relation of the quarks will be modified as,

$$E_f(B) = [M_f^2 + p_z^2 + (2l+1-s)|q_f|B]^{1/2}, \tag{4}$$

where M_f is the effective quark mass for a quark of flavour f. The magnetic field is in the z direction ($\vec{B} = B\hat{z}$), which results in discretising the momentum in the transverse plane, here in the $x-y$ plane. The transverse component of the

momentum now depends on both the Landau level (LL), l and the spin, s. It is important to note how in the magnetised version the energy of the individual flavour is dependent not only on the respective effective masses but also on the respective charges. Another important change, which is somewhat expected from Eq. 4, is in the integral over the three momenta,

$$\int \frac{d^3p}{(2\pi)^3} \to \frac{|q_f|B}{2\pi} \sum_{l=0}^{\infty} \int_{-\infty}^{\infty} \frac{dp_z}{2\pi}. \tag{5}$$

The integral is now performed only over the continuous component, p_z. Also, note the change in the lower limit of the integral as compared to the zero magnetic field case, where it is 0.

With all these knowledge in hand, we can get the thermodynamic potential potential for the NJL model in presence of the magnetic field as,

$$\Omega^B_{\rm NJL}(T,\mu) = G_S \sum_{f=u,d,s} \sigma_f^2 - 4G_D\sigma_u\sigma_d\sigma_s + \sum_{f=u,d,s} \left(\Omega^f_{\rm mev} + \Omega^f_{\rm med}\right) + \frac{B^2}{2}, \tag{6}$$

where, $\sigma_f = \langle\bar{\psi}_f\psi_f\rangle$ with $f = u$, d and s.[1] The first two terms are the vacuum contributions from the condensates of different flavours. The second term arises from the 't Hooft determinant term and is the explicit manifestation of preservation of the axial anomaly. $\Omega^f_{\rm mev}$ is a term which we call magnetic field entangled vacuum term. It can be separated into a purely magnetic field dependent term and the standard vacuum term, which we show in a moment. $\Omega^f_{\rm med}$ is the term in presence of both the magnetic field and the temperature and can be termed as the medium term.

These two terms are given as,

$$\Omega^f_{\rm mev} = -\frac{N_c}{2\pi} \sum_{f,l,s} |q_f|B \int_{-\infty}^{\infty} \frac{dp_z}{(2\pi)} E_f(B) \quad \text{and} \tag{7}$$

$$\Omega^f_{\rm med} = -\frac{N_c}{2\pi} T \sum_{f,l,s} |q_f|B \int_{-\infty}^{\infty} \frac{dp_z}{(2\pi)} \left[\ln\left(1 + e^{-(E_f(B)-\mu)/T}\right) + \ln\left(1 + e^{-(E_f(B)+\mu)/T}\right)\right], \tag{8}$$

respectively. f, l and s stand for the summation over flavour, Landau levels and spin states of the quarks, respectively. Following the technique in Ref. [41], $\Omega^f_{\rm mev}$ can be further decomposed into the standard vacuum term ($\Omega^f_{\rm vac}$) and a purely magnetic field dependent term ($\Omega^f_{\rm mag}$), $\Omega^f_{\rm mev} = \Omega^f_{\rm vac} + \Omega^f_{\rm mag}$, as

$$\Omega^f_{\rm vac} = -2N_c \int_{\Lambda} \frac{d^3p}{(2\pi)^3} E^f_p \quad \text{and} \tag{9}$$

$$\Omega^f_{\rm mag} = -\frac{N_c}{2\pi^2} \sum_f (|q_f|B)^2 \left(\zeta'(-1,x_f) + \frac{x_f^2}{4} - \frac{1}{2}(x_f^2 - x_f)\ln x_f\right), \tag{10}$$

where $E^f_p = \sqrt{M_f^2 + p^2}$ is the particle energy in vacuum,[2] $x_f = M_f^2/(2|q_f|B)$ and $\zeta'(-1,x_f) = d\zeta(z,x_f)/dz|_{z=-1}$ with $\zeta(z,x_f)$ is the Riemann-Hurwitz zeta function. The detail of obtaining the expression for $\Omega_{\rm mag}$ can be found in Ref. [41].

Thus, the final expression for the thermodynamic potential in NJL model becomes,

$$\Omega^B_{\rm NJL}(T,\mu) = G_S \sum_{f=u,d,s} \sigma_f^2 - 4G_D\sigma_u\sigma_d\sigma_s + \sum_{f=u,d,s} \left(\Omega^f_{\rm vac} + \Omega^f_{\rm mag} + \Omega^f_{\rm med}\right) + \frac{B^2}{2}. \tag{11}$$

We take the model parameters as: Number of light flavours = 2, number of colours = 3, $m_u = m_d = 0.0055$ GeV, $m_s = 0.1407$ GeV, three momentum cut-off $\Lambda = 0.6023$ GeV, the scalar coupling constant,[3] $G_S = 3.67/\Lambda^2$, the coupling constant for the 't Hooft determinant term, $G_D = 12.36/\Lambda^5$, pion mass $m_\pi = 0.135$ GeV and the pion decay constant, $f_\pi = 0.0924$ GeV (0.0879 GeV, in the chiral limit), kaon mass $m_k = 0.4977$ GeV, eta mesons, $m_\eta^{'} = 0.9578$ GeV and $m_\eta = 0.5148$ GeV. All these parameters are taken from the Ref. [51].

The magnetic field dependent coupling constant is fitted as [33],

$$G_S(\xi) = G_S^0 \frac{1 + a\xi^2 + b\xi^3}{1 + c\xi^2 + d\xi^4}, \tag{12}$$

where, $a = 0.0108805$, $b = -1.0133 \times 10^{-4}$, $c = 0.02228$, $d = 1.84558 \times 10^{-4}$; $\Lambda_{QCD} = 0.3$ GeV, $\xi = eB/\Lambda^2_{QCD}$ and $G_S^0 = G_S(eB = 0) = G_S$.

[1] Please note that the second term in the potential has a opposite sign in Ref. [33]. That's a typo. Our sign matches with Ref. [50,51].

[2] One should note that just by putting $B = 0$ in Eq. 4 the vacuum dispersion relation cannot be recovered.

[3] Note that the value of G_S quoted here or in Ref. [33] is double the value given in Refs. [50,51]. This is because of the the definition of the coupling constant G_S. It appears in the Lagrangian here (or in Ref. [33]) with a factor of 1/2 in contrast to just G_S in Refs. [50,51].

Because of the 't Hooft determinant term there is a cross-flavour coupling which is called "flavour mixing" [50]. As a result the effective masses are given by

$$\begin{aligned} M_u &= m_u - 2G_S\sigma_u + 2G_D\sigma_d\sigma_s\,, \\ M_d &= m_d - 2G_S\sigma_d + 2G_D\sigma_u\sigma_s \quad \text{and} \\ M_s &= m_s - 2G_S\sigma_s + 2G_D\sigma_u\sigma_d, \end{aligned} \tag{13}$$

for up, down and strange quarks, respectively.

2.2 Nonextensive statistics

We know that the entropy is considered to be an extensive property, i.e., its value depends on the system size. Constantino Tsallis proposed a nonextensive statistics [16], which provides a generalisation of the traditional BG entropy. This generalisation is made through a parameter q, which, in the limit $q \to 1$, gives back the BG entropy.

As compared to the exponentials in traditional extensive statistics, the nonextensive statistics lead to power laws. This is the most fundamentally different manifestation of the entropy being a nonextensive quantity.

Mathematically speaking, in nonextensive statistics or the so-called Tsallis statistics, the usual exponential are replaced by an equivalent q-exponential,

$$\exp\left(-\frac{E}{T}\right) \to \exp_q\left(-\frac{E}{T}\right), \tag{14}$$

where,

$$\exp_q(x) \equiv \begin{cases} \left(1+(q-1)x\right)^{1/(q-1)}, & \text{if } x > 0 \\ \left(1+(1-q)x\right)^{1/(1-q)}, & \text{if } x \leq 0. \end{cases} \tag{15}$$

Using these expressions one can get the generalised versions of the standard statistical distributions. One can derive the Tsallis distribution starting from the Boltzmann equation [52]. It is straightforward to check that the above equation reduces to the standard exponential in the limit $q \to 1$ giving back the standard distributions. Any values of q other than unity gives a measure of the "nonextensiveness" of the system. In the same fashion the inverse function, i.e., the equivalent to standard logarithm can as well be defined,

$$\ln_q(x) \equiv \begin{cases} \frac{x^{q-1}-1}{q-1}, & \text{if } x > 0 \\ \frac{x^{1-q}-1}{1-q}, & \text{if } x \leq 0. \end{cases} \tag{16}$$

It can be again trivially checked that this reduces to the standard logarithmic function of the variable x in the limit $q \to 1$.

Now, we will introduce the NJL model for a nonextensive statistics. In that case, only Ω^f_{med} will be modified from the expression of the full thermodynamic potential given in Eq. 11. Ω^f_{med} is given in Eq. 8. It is evident that the logarithms in that equation will be modified to incorporate the nonextensive parameter q. This will be done using Eqs. 15 and 16.

For the analysis in the nonextensive scenarios, we assume that there will not be any modifications to the model parameters due to the nonextensive nature of the system. So, the treatment of the nonextensive parameter q will be in the same footing as the temperature and chemical potential in the model. The model parameters fitted at zero temperature and chemical potential are used to evolve the system at nonzero temperature and chemical potential. The guideline for q remains the same. We extend this argument further in the presence of the magnetic field and the treatment of the magnetised medium remains analogous.

The modification in Eq. 8 can be summarised as,

$$\begin{aligned} \Omega^f_{\text{med},q} = -\frac{N_c}{2\pi}T\sum_{f,l,s}|q_f|B\int_{-\infty}^{\infty}\frac{dp_z}{(2\pi)} \\ \left[\ln_q\left(1+e_q^{-(E_f(B)-\mu)/T}\right)\right. \\ \left.+\ln_q\left(1+e_q^{-(E_f(B)+\mu)/T}\right)\right]. \end{aligned} \tag{17}$$

In the present analysis, we stick to the zero chemical potential scenario.[4] In that case, ensuring $e_q(x)$ to be always a real number the condition $\left(1+(1-q)x\right)^{1/(1-q)} \geq 0$ has to be satisfied. Considering $q > 1$ always satisfies the condition. On the other hand, q-values > 1 are also phenomenologically well motivated [12,24], which we elaborate in the result section.

3 Results

3.1 In the absence of a magnetic field

To explore the properties of a nonextensive magnetised medium we begin by revisiting the scenario in the absence of an external field. To meet that purpose we employ a $2+1$-flavour NJL model. We are more interested to explore the QCD phase diagram. Thus, chiral dynamics will hold the central attention while we utilise the NJL model.

In the upper panel of Fig. 1, we show the plots of condensates for up/down (left panel) and strange (right panel) quarks as a function of T for different values of the nonextensive parameter q. We observe that the chiral condensates decreases with increasing nonextensivity around the transition region. The transition also tends to be sharper for both

[4] It should be noted that the formulation of the nonextensive statistics is not unique when one needs to deal with both particles and antiparticles for fermions [28].

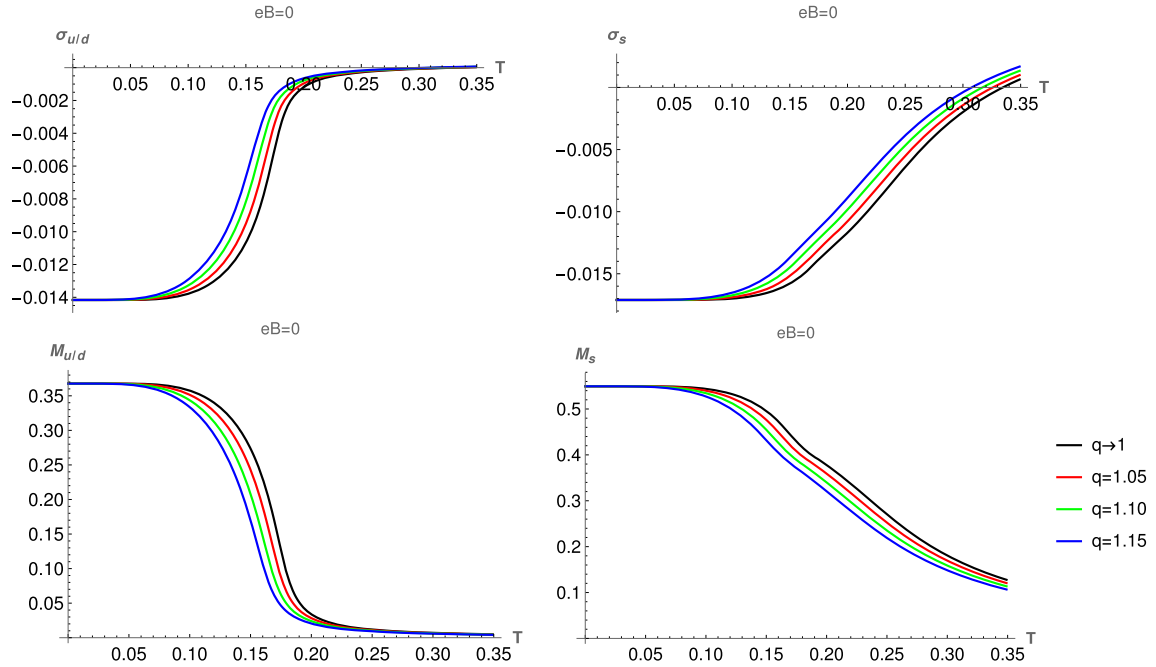

Fig. 1 ($\boldsymbol{B = 0}$): Plot of the condensates (upper panel) and effective masses (lower panel) for different values of the q parameter. Left panel: light quarks. Right panel: strange quark

the light and heavy quarks. Eventually, we will be more focussed on the fate of the light quarks. The plots of the strange quark condensates are displayed to keep track of the heaviest constituent of the system. To obtain the plots for the corresponding effective masses is straightforward (Eq. 13) and they reflect the same decreasing behaviour as the quark condensates with increasing q values as shown in the lower panel of Fig. 1. Such weakening of chiral condensates and effective masses when the medium departs from its extensive nature agree with existing results [27,29].

For the choice of $q > 1$, in principle, one can take any higher values but in practice, it is never far away from unity, particularly in the case of HICs. In such experiments, typical values of q obtained from the fits to the transverse momentum distribution for identified charged particles lies within the range of $1.1 - 1.2$ [12,24]. Thus, the maximum deviation of q should not exceed 20%. Keeping this in mind we have taken three different values of q, 1.05, 1.10 and1.15 to illustrate the effect of "nonextensiveness"; with the highest value remaining well within the expected limit.

In Table 1, we quote the transition temperatures ($T_{\rm CO}$) as a function of q. They are obtained by tracking the inflection points of the condensates. The quoted numbers are only for the light quarks (same for both up and down quarks). To have a pictorial idea of the decrease in chiral transition temperature, we show a plot of the $T_{\rm CO}$ as a function of q with the $T_{\rm CO}$ being scaled with $T_{\rm CO}(q = 1)$ in Fig. 2. There is roughly 10 percentage decrease in the transition temperature for the highest value of q that we consider here.

Table 1 ($\boldsymbol{B = 0}$): Chiral transition temperature as a function of q

q	1	1.05	1.10	1.15
$T_{\rm CO}$ (MeV)	173	168	162	156

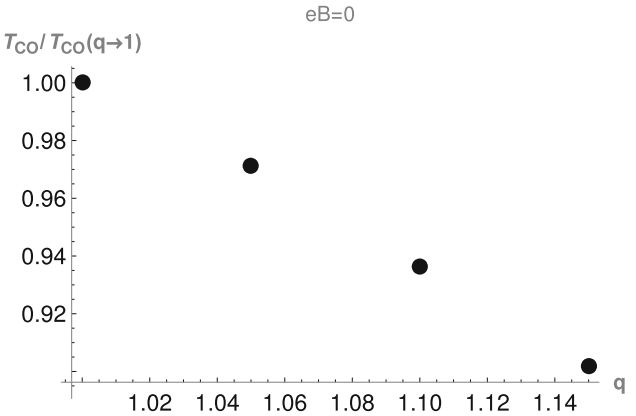

Fig. 2 ($\boldsymbol{B = 0}$): Scaled $T_{\rm CO}$ as a function of q

3.2 In the presence of a magnetic field

In the pursuit of exploring the magnetised nonextensive medium, we proceed chronologically, i.e., we follow the steps how the NJL model in presence of the magnetic field has been developed over the years. Thus, we start with the constant G_S. In that case, the NJL model is known to produce the effect of MC throughout the temperature range [53,54].

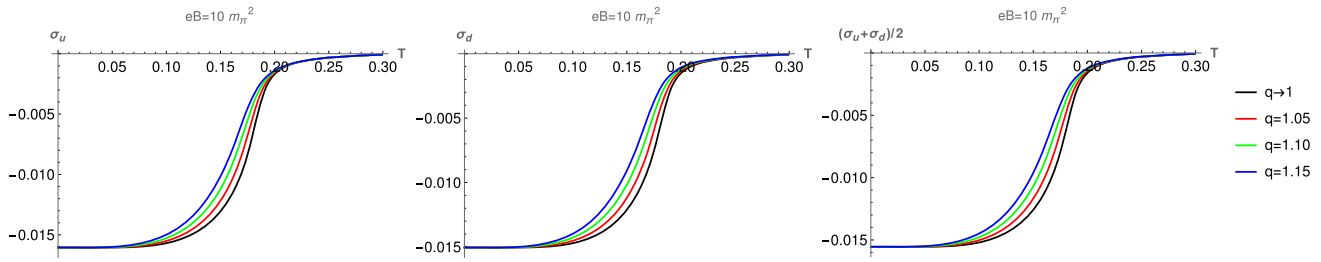

Fig. 3 $(B \neq 0, G_S^0)$: Plot of the condensates for different values of q at $eB = 10\ m_\pi^2$. First two panels show up and down quark condensates, respectively. The last panel is for condensate average

Table 2 (G_S^0): Chiral transition temperature as a function of q for $eB = 10\, m_\pi^2$

q	1	1.05	1.10	1.15
T_{CO} (MeV)	182	177	172	167

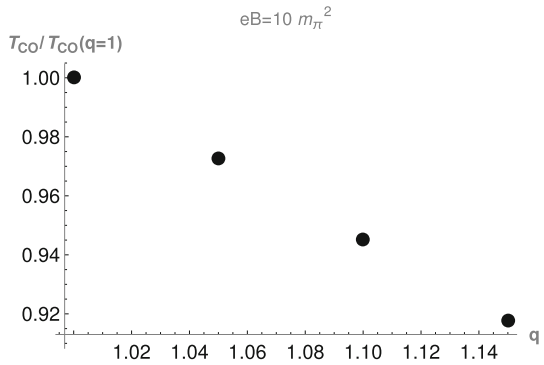

Fig. 4 (G_S^0): Scaled T_{CO} as a function of q for $eB = 10\, m_\pi^2$

It is interesting to check how the magnetised nonextensive medium behaves with a constant coupling.

After the discovery of the IMC effect by LQCD [5], effective models were tweaked to reproduce that effect. One of the ways in the NJL model is to make the coupling constant dependent on eB [33] or on both eB and T [32,35]. In our present study, we choose to work with the parametrisation given in [33]. The parametric form solely depends on eB and there is no involvement of temperature.

Since we will discuss (I)MC effects in detail, we should define them appropriately and leave no scope for confusion. The MC or IMC is always defined by looking at the behaviour of the condensates —, its increasing value signifies catalysis and decreasing value implies to inverse catalysis. The trend of T_{CO} plays no role there. It is a coincidence that for the physical parameters IMC effect is accompanied with a decreasing T_{CO}. In fact, one can conjure up scenarios in which the condensate values enhance (thus MC) but the T_{CO} still decreases [55].

Apart from the NJL model [32,33,35,46], there are other effective models which have been utilised to study QCD in presence of a magnetic field. For example, linear sigma model (LSM) with quarks is used to explore the IMC effect in Ref. [34], whereas its Polyakov loop extended version (PLSM) and hadron resonance gas (HRG) models are utilised to explore thermodynamic quantities like magnetisation etc in Ref. [36]. PLSM model has also been used further in the presence of magnetic field in Refs. [37–39].

3.2.1 *Constant coupling*

With the constant coupling, we begin the discussion by showing the plots of uniquely $(10\ m_\pi^2)$ magnetised condensates for different values of the q parameter in Fig. 3. Because of their different coupling strength to the magnetic field the up and down quark condensates are now different. They are shown in the first and second panel. The overall effect of increasing q value remains the same as it is in zero eB case (Fig. 1), i.e., the condensate decreases with increasing q for a given value of T. In the third panel, we describe the condensate average with the same criteria. It is important as it will be used to define the chiral crossover temperature[5] as well as the the fate of (I)MC will be decided by looking at its behaviour. On the other hand, to track the behaviour of the individual quark condensate is important, as they respond differently in the presence of a magnetic field.

The values of the T_{CO} for different values of q are given in Table 2. As expected from the behaviour of the condensates, T_{CO} decreases as a function of q. To understand the percentage decrement, we provide with a scaled T_{CO} plot in Fig. 4. The reduction in the crossover temperature can be as high as 10% for the highest used value of q.

If the extent of the nonextensivity of the medium is fixed and the magnetic field is varied then the effects on the condensates are shown in Fig. 5. For the sake of comparison, the scenarios for the extensive case are also shown with the dashed lines with increasing strength of the magnetic field. The known MC effect is evident there. The MC effect also prevails in the nonextensive medium with two noticeable

[5] It is important to note that the crossover temperatures for the two light quarks may not coincide with a broken isospin symmetry.

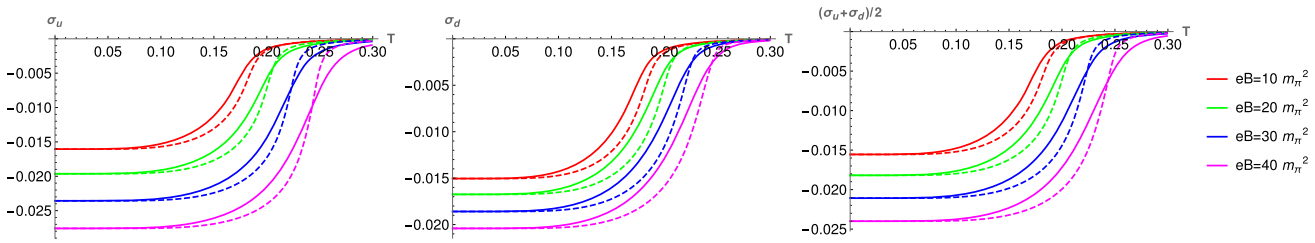

Fig. 5 $(B \neq 0, G_S^0)$: Plot of the condensates for different values of eB for both extensive ($q \to 1$; dotted lines) and nonextensive ($q = 1.1$; solid lines) cases. The three panels represent up, down and average condensates, respectively

Table 3 (G_S^0): Chiral transition temperature for different values of eB and q

eB (m_π^2)		0	10	20	30	40
T_{CO} (MeV)	$q \to 1$:	173	182	200	222	244
	$q = 1.10$:	162	172	192	213	231

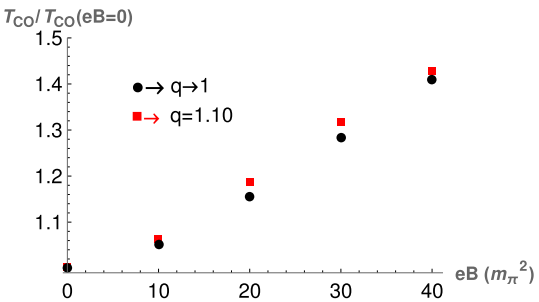

Fig. 6 (G_S^0): Scaled T_{CO} as a function of eB

differences. First, at a given eB value, the strength of the condensate for $q = 1.1$ is smaller than the extensive case, particularly in the vicinity of the transition region. In fact, it is within this transition region that the differences between the extensive and nonextensive media are most conspicuous, especially when dealing with lower magnetic field values. Secondly, the fall of the curves are comparatively flattened in a nonextensive medium. These affect the fate of the chiral dynamics of the system which we discuss next.

With MC prevailing for both extensive and nonextensive cases, the weakening of the chiral condensates and the corresponding transition temperatures are evident in Fig. 5. This is what reflects in the Table 3, where we provide T_{CO}'s for both $q \to 1$ and $q = 1.10$ with different values of eB. Though the T_{CO} for a given value of eB is smaller for a nonextensive medium as compared to the extensive one, the percentage change is always higher for the former for all values of eB considered here. It is depicted in Fig. 6, where the T_{CO}'s are scaled with the respective values at zero eB.

3.2.2 *Magnetic field dependent coupling constant*

For the field dependent coupling constant, we first show the condensate plots for the light quarks along with the average for the known extensive scenario. It is important to note that we are not using the modified definition of the condensates utilised in Ref. [33] (Eq.14) which are taken from LQCD [5]. Such definitions are particularly used in effective models to have results on the same footing and thus comparable with that in LQCD.

In the present study, we do not have such obligation as we are not comparing with any existing data. Rather, we are interested to investigate the fate of the (I)MC effects for a nonextensive medium in the model itself. Thus for us, knowing the condensates and their average will be adequate to decide on the fate of the (I)MC effects and the trend of T_{CO}. To determine the nature of the effect (whether MC or IMC) the condensate averages will be sufficient as argued in the third paragraph of Sect. 3.2.

Before going to discuss the results a few comments are necessary. In Ref. [40], it was shown that the coupling constant decreases with the increasing magnetic field strength as $\alpha_s(eB) = 1/\left(b \ln(|eB|/\Lambda^2_{QCD})\right)$, where α_s is the strong interaction coupling constant and $b = (11N_c - 2N_f)/6\pi$. If we consider G_S to be analogous to α_s, then it should as well decrease with eB. Thus, this form can be used as an ansatz to model the running coupling in NJL model. Since, we plan to make this study an extensive one, we explore this possibility as well and put it in the Appendix IV.

In Fig. 7, the condensates in an extensive medium with a magnetic field dependent coupling constant are plotted. It is evident from the plots that IMC effect, expectedly, prevails around the transition region. This is similar to what is found in the existing literatures [32,32,33,33–35,35–39,46]. Though the status of IMC will be finally decided by the trend of the condensate average, it is also interesting to observe the individual flavour. What we notice is that the up and down quarks are not affected by the IMC effect with equal magnitude. This comes as no surprise considering the different coupling strengths of up and down quarks with the magnetic field. In fact, if one calculates the crossover tempera-

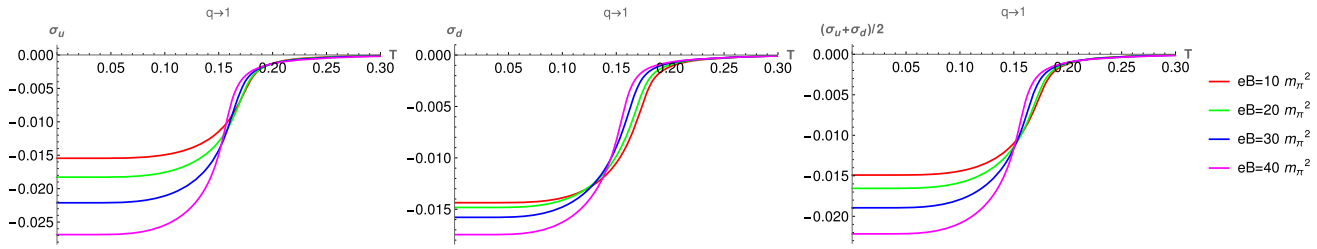

Fig. 7 $(B \neq 0, G_S(eB))$: Plot of the light quark condensates and their averages for different values of eB for the extensive medium. Left to right panels represent up, down and average condensates, respectively

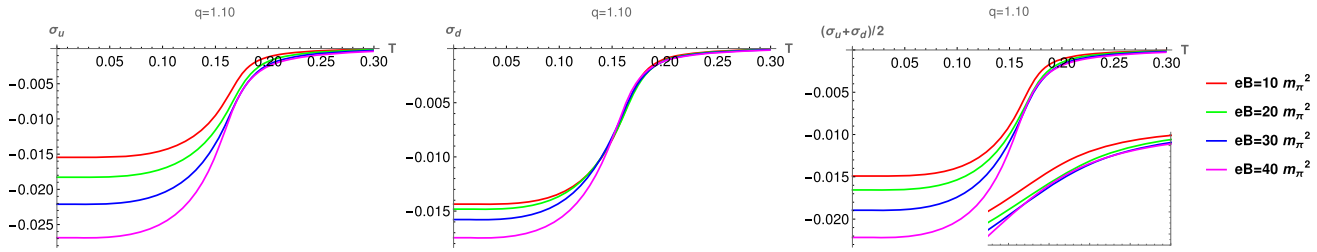

Fig. 8 $(B \neq 0, G_S(eB))$: Plot of the condensates and their averages for different values of eB in a nonextensive medium. Panels are designated in the same way as in Fig. 7

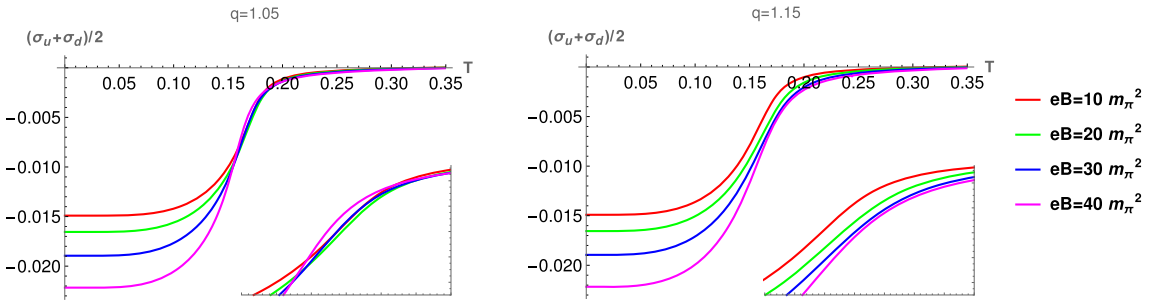

Fig. 9 $(B \neq 0, G_S(eB))$: Plot of the condensate averages for different values of eB with two different q's: $q = 1.05$ (left panel) and $q = 1.15$ (right panel)

ture for individual flavour, they will be different. Though, as already mentioned, the crossover temperature that we quote will always be obtained using the condensate average. It will be interesting to study how these scenarios are affected in a nonextensive medium, which we discuss next.

In Fig. 8, we show the same plots as those in Fig. 7 but for a nonextensive medium with $q = 1.10$. We observe some interesting changes in the behaviour of the individual as well as the average condensates. It is clear that the IMC effect for up quark is spoiled for all the strengths of the magnetic field considered here. For the down quark, the effect is present almost for all values of eB but with a reduced strength. Thus, two light quarks, expectedly, behave differently in presence of a magnetic field. As for the condensate average, which we use to decide on the types of the effect in the medium, the IMC effect is ruined by the "nonextensiveness" of the medium except for the highest strengths of eB considered here. This is elaborated with an inset plot zooming in the crossing regions. It is obvious that there is an interplay between the strengths of q and eB, which eventually determines the types of catalysing effects (MC or IMC). We elaborate it with the next two figures.

Table 4 $(B \neq 0, G_S(eB))$: Chiral transition temperature for different values of eB and q

eB (m_π^2)		0	10	20	30	40
T_{CO} (MeV)	$q \to 1$:	173	173	169	163	156
	$q = 1.05$:	168	168	168	163	157
	$q = 1.10$:	162	164	165	162	157
	$q = 1.15$:	156	159	162	160	156

In Fig. 9, we plot the condensate averages for different values of eB with two different values of q. These two figures help us understand the interplay between eB and q on determining the types of the catalysing effects in the medium. For $q = 1.05$, the IMC effect reappears starting from $eB = 30\,m_\pi^2$ as shown in the figure in the left panel.

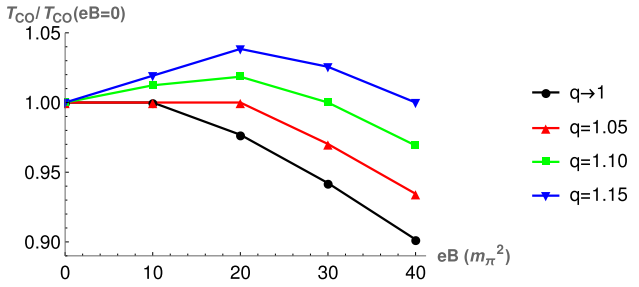

Fig. 10 $(B \neq 0, G_S(eB))$: Scaled T_{CO} as a function of eB

Thus, decreasing q from 1.10 to 1.05 makes the IMC effect favourable for lower values of eB. On the other hand, if we increase q to 1.15 the IMC effect completely disappears as evident from the figure in the right panel. For both the panels, the transition regions are zoomed in for the inset plots to make the crossings of the condensates conspicuous.

Now, we make a comparison of the T_{CO}'s for different values of q including the extensive case with zero magnetic field in Table 4. For $q \to 1$, the decreasing nature of the crossover temperature is captured. As we crank up the nonextensive nature of the medium by increasing q, T_{CO} starts behaving differently. For $q = 1.05$, Initially it does not change and then it decreases with increasing eB. With further increase in q the trend becomes non-monotonic. For both $q = 1.10$ and 1.15, T_{CO} first increases and then decreases. With higher q values the increase is greater.

All these points are well illustrated in the Fig. 10, where we can also read out the percentage change in the crossover temperatures and their trend following the liens which are solely intended to guide the eyes. We also observe that decreasing T_{CO} is not always accompanied with IMC. For example, at $q = 1.15$ the IMC effect is absent but we still observe decreasing T_{CO} for the higher values of eB. Thus, simultaneous occurrence of the two is a mere coincidence as has been discussed in detail in Ref. [55]. There it is shown that with higher pion masses there is MC effect but with decreasing T_{CO}.

It is also noteworthy that such non-monotonic behaviors arise in the context of an effective model due to the interplay between eB and q, with $q \geq 1.10$. Such q-values render the medium non-extensive. On the other hand, all the available LQCD studies [6,56,57] demonstrate a monotonic decreasing behaviour of the crossover temperature as a function of the magnetic field, which are obviously based on extensive thermodynamics.

Finally, in Fig. 11 we show the plots for the condensates for different values of q with a given eB. This is analogous to Fig. 3 but for a varying coupling constant. The condensates along with their averages still display the decreasing features below the T_{CO}'s with increasing q values just like Fig. 3 with a crossing just above the transition temperatures. This crossing appears because of the running coupling constant.

In Table 5, we quote the T_{CO} values for different q at $eB = 20\, m_\pi^2$. It is not affected by the crossings of the condensates and decreases with increasing q as in the case with a constant coupling. In Fig. 12, the scaled transition temperature is shown as a function of q to elucidate the percentage change.

4 Conclusion

We have presented an NJL model analysis of a magnetised QCD medium in a nonextensive ambience. There exist study discussing chiral symmetry restoration and other properties like meson masses in such scenarios. We add to that ongoing effort by including the magnetic field.

To achieve our goal, we utilised a 2+1 flavour NJL model. We start the analysis by revisiting the zero magnetic field case and found that the strength of the chiral condensate decreases with increasing nonextensive parameter q. With increasing q the chiral transition temperature decreases as well. These findings are in accord with what we already know and put our study into a perspective.

While coming to the focal point of the present work, we include the magnetic field and investigate the chiral transition for a q-value greater than unity. We also analysed and discussed the results for $q \to 1$ wherever deemed necessary. The analysis is mainly divided into two parts — with (i) a constant coupling (G_S^0) and (ii) a magnetic field dependent coupling constant ($G_S(eB)$).

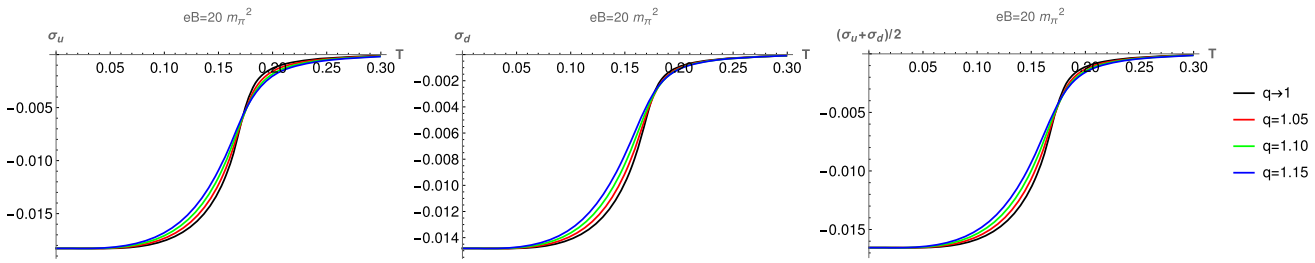

Fig. 11 $(B \neq 0, G_S(eB))$: Plot of the condensates and their averages for different values of the q parameter. Left to right panels represent up quark, down quark and average condensates, respectively

Table 5 ($B \neq 0$, $G_S(eB)$): Chiral transition temperature as a function of q for $eB = 20\,m_\pi^2$

q	1	1.05	1.10	1.15
T_{CO} (MeV)	169	168	165	162

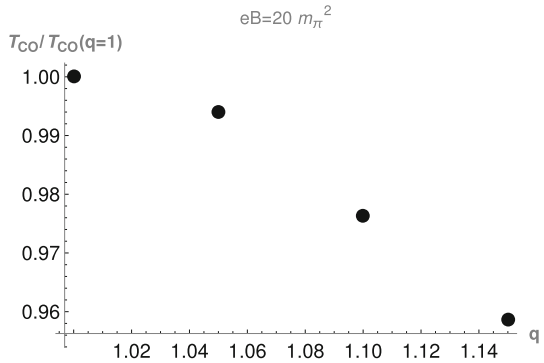

Fig. 12 ($B \neq 0$, $G_S(eB)$): Scaled T_{CO} as a function of q for $eB = 20\,m_\pi^2$

For a constant coupling at a specific magnetic field strength, the impact of increasing q resembles that of the zero magnetic field case, leading to a decreasing trend in both the condensates and the transition temperatures. The well-known magnetic catalysis effect persists with increasing eB for a q-value greater than unity. However, it results in reduced strength in both the condensates and the transition temperatures compared to the extensive scenario. We also discovered that the percentage increase in the transition temperatures is consistently higher in a nonextensive scenario.

For a magnetic field dependent coupling the observations are more interesting. Depending on the strength of q and eB the observed IMC effect in BG statistics can be destroyed. For $q = 1.10$, the IMC effect, which is nothing but the decreasing condensates with increasing strength of eB, is missing, except for the highest strength of magnetic field ($40m_\pi^2$) that we examined in this study.

There is a competition between the two parameters q and eB which becomes evident when we analysed for other two values of $q = 1.05$ and 1.15. For $q = 1.05$, the IMC effect can be observed for $eB = 30m_\pi^2$, a field value lower than that required for $q = 1.10$. On the other hand, at $q = 1.15$, the IMC effect is totally eliminated for all the strengths of eB explored here.

With eB-dependent G_S the behaviour of the transition temperature, argued to be independent of the IMC effect, turns out to be little subtle. It also depends on both q and eB. For $q = 1.05$, it remains constant initially and then starts decreasing with increasing magnetic field. At even higher values of q, it exhibits a non-monotonic trend as a function of eB — initially increasing before subsequently starts falling. The initial increment is higher for higher values of q.

We also explored the condensates using $G_S(eB)$ for different values of q with a given eB. There is a crossing of the condensates at a temperature slightly higher than the transition temperature as compared to no-crossing with constant G_S. Also, in this case, the percentage decrease of the transition temperature is slightly lower as compared to the constant G_S.

However, we must keep in mind that the temperature in Tsallis statistics can have a more generalised meaning due to its non-extensive nature. In this regard, using a more generalised statistics [58,59] could be useful. Such a statistics is characterised by a unique pair of scaling exponents and the Tsallis statistics along with the Boltzmann-Gibbs statistics become special cases. It has been recently utilised in Ref. [60] to successfully reproduce the particle ratios at two different energies in HICs. There exist other works [61,62] along with a review on the topic [63]. Thus, it will be interesting to check how much of the present conclusion gets affected in such a generalised scenario and demands a separate investigation.

Having discussed these interesting findings within a mean-field approach, it becomes intriguing to explore the effects of fluctuations by transitioning to beyond mean-field approximations. In the pursuit of robust predictions, it will be interesting to test some of the present observations using beyond mean field approaches. For example, the weakening of the chiral condensates with increasing q parameter, the non-monotonic behaviour of the T_{CO} as a function eB for q-values greater than unity etc. Such exercises are certainly beyond the scope of the present study and will be reported elsewhere.

As an immediate extension to the present analysis of the chiral symmetry for a nonextensive magnetised medium it would be really interesting to include the background gauge field to bring out the effect of statistical confinement. This will be particularly useful in the investigation of transport properties [64,65] with effective degrees of freedom following the technique outlined in [66]. Such investigations could bear implications for HIC related observations. It also remains to be seen whether, by employing the techniques outlined in Ref. [67], the findings of the present effective model can be linked to certain phenomenological consequences. We plan to report on these in the near future.

Acknowledgements The author would like to thank Aritra Das working with whom on a different project makes him eligible to write faster and efficient codes for the present work. This research was supported in part by the ExtreMe Matter Institute EMMI at the GSI Helmholtzzentrum fuer Schwerionenforschung GmbH, Darmstadt, Germany.

Funding Open Access funding enabled and organized by Projekt DEAL.

Data Availability Statement Data will be made available on reasonable request. [Author's comment: The data for the current study will be made available from the corresponding author on reasonable request.].

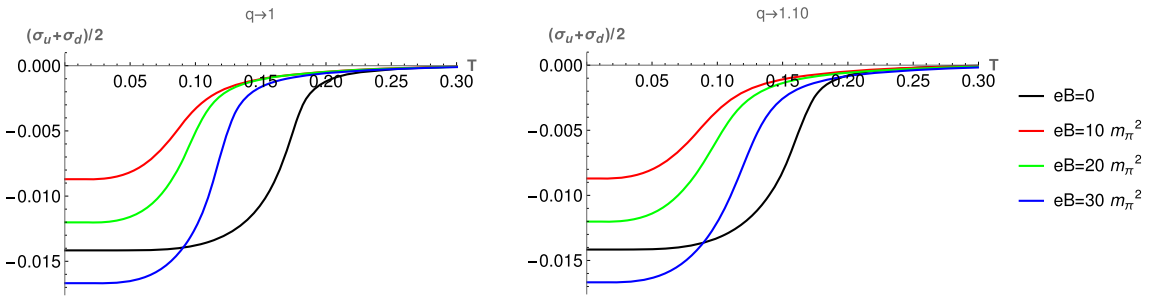

Fig. 13 $(G_S^0/G_S(eB))$: Plot of the condensate averages for different values of eB both in the extensive (left panel) and nonextensive (right panel) scenarios

Code Availability Statement Code/software will be made available on reasonable request. [Author's comment: The code/software generated during and/or analysed during the current study is available from the corresponding author on reasonable request.].

Appendices

A Magnetic field dependent coupling constant (simple ansatz)

The main motivation behind the discussion in this appendix is to make the present study exhaustive and explore all possible directions that have been investigated for an extensive magnetised QCD medium using an effective model like NJL. If we follow the argument given in [33,40], then G_S becoming a decreasing function of eB becomes an obvious fact. We exploit their argument and using the ansatz in Ref. [33] introduce a magnetic field dependent coupling constant

$$G_S(eB) = G_S^0/\ln(e + |eB|/\Lambda_{\rm QCD}^2). \tag{18}$$

In case of a very high value of the magnetic field the coupling constant vanishes and bringing the magnetic field down to zero gives us back G_S^0.

We explore this particular form to see its effect. We only focus on the condensate average to decide on the types of the catalysing effects and the transition temperatures. It is evident from Fig. 13 that with this simple ansatz (Eq. 18) of decreasing coupling constant as a function of eB one can get the IMC effect up to certain value of eB albeit inconsistently.

Upon concentrating on the left panel, we learn that for smaller values of magnetic field the condensate values remain always below that of zero eB value. Also, the condensates with nonzero eB values do not reflect the IMC effect among themselves. The crossover temperature at non-zero eB values decreases initially and then starts increasing with increasing eB. The $T_{\rm CO}$'s, up to the values we have explored here, always remain below that in zero magnetic field case. These are in conformity with the observation in Ref. [33]. Thus, though this simple ansatz can provide a hint of IMC effect and decreasing $T_{\rm CO}$ it fails to be in accord with the established evidence [5,6]. It is useful as a hint and needs to be tweaked to be successfully used in an effective model [32,33,35].

As we extend this analysis for a nonextensive medium ($q = 1.10$), no important change is observed and the discussion in the above paragraph remains more or less valid. The only change that takes place is the reduction in the gap of $T_{\rm CO}$'s between the zero eB and highest value of eB considered. Thus we can safely conclude that the magnetic field dependent coupling constant with a simple ansatz does not behave much differently in a nonextensive medium.

References

1. V. Skokov, A.Y. Illarionov, V. Toneev, Int. J. Mod. Phys. A **24**, 5925 (2009). https://doi.org/10.1142/S0217751X09047570. arXiv:0907.1396 [nucl-th]
2. D. Kharzeev, K. Landsteiner, A. Schmitt, H.-U. Yee, eds., *Strongly Interacting Matter in Magnetic Fields*, Vol. 871 (Springer, 2013)https://doi.org/10.1007/978-3-642-37305-3
3. V.A. Miransky I.A. Shovkovy, Phys. Rept. **576**, 1 (2015), https://doi.org/10.1016/j.physrep.2015.02.003; arXiv:1503.00732 [hep-ph]
4. V.P. Gusynin, V.A. Miransky, I.A. Shovkovy, Phys. Rev. Lett. **73**, 3499 (1994), [Erratum: Phys.Rev.Lett. 76, 1005 (1996)], https://doi.org/10.1103/PhysRevLett.73.3499 arXiv:hep-ph/9405262
5. G.S. Bali, F. Bruckmann, G. Endrodi, Z. Fodor, S.D. Katz, A. Schafer, Phys. Rev. D **86**, 071502 (2012). https://doi.org/10.1103/PhysRevD.86.071502. arXiv:1206.4205

6. G.S. Bali, F. Bruckmann, G. Endrodi, Z. Fodor, S.D. Katz, S. Krieg, A. Schafer, K.K. Szabo, JHEP **02**, 044 (2012). https://doi.org/10.1007/JHEP02(2012)044. arXiv:1111.4956
7. K. Fukushima, D.E. Kharzeev, H.J. Warringa, Phys. Rev. D **78**, 074033 (2008). https://doi.org/10.1103/PhysRevD.78.074033. arXiv:0808.3382
8. D.T. Son A.R. Zhitnitsky, Phys. Rev. D **70**, 074018 (2004),https://doi.org/10.1103/PhysRevD.70.074018. arXiv:hep-ph/0405216
9. M.A. Metlitski A.R. Zhitnitsky, Phys. Rev. D **72**, 045011 (2005),https://doi.org/10.1103/PhysRevD.72.045011. arXiv:hep-ph/0505072
10. D.E. Kharzeev, J. Liao, S.A. Voloshin, G. Wang, Prog. Part. Nucl. Phys. **88**, 1 (2016). https://doi.org/10.1016/j.ppnp.2016.01.001. arXiv:1511.04050
11. A. Adare et al., PHENIX. Phys. Rev. C **83**, 064903 (2011). https://doi.org/10.1103/PhysRevC.83.064903. arXiv:1102.0753
12. K. Aamodt et al., ALICE. Eur. Phys. J. C **71**, 1655 (2011). https://doi.org/10.1140/epjc/s10052-011-1655-9. arXiv:1101.4110
13. V. Khachatryan et al., CMS. JHEP **05**, 064 (2011). https://doi.org/10.1007/JHEP05(2011)064. arXiv:1102.4282
14. R.N. Patra, B. Mohanty, T.K. Nayak, Eur. Phys. J. Plus **136**, 702 (2021). https://doi.org/10.1140/epjp/s13360-021-01660-0. arXiv:2008.02559
15. G.S. Pradhan, D. Sahu, R. Rath, R. Sahoo, J. Cleymans, Eur. Phys. J. A **60**, 52 (2024). https://doi.org/10.1140/epja/s10050-024-01270-1. arXiv:2301.04038
16. C. Tsallis, J. Statist. Phys. **52**, 479 (1988). https://doi.org/10.1007/BF01016429
17. C. Tsallis, Introduction to Nonextensive Statistical Mechanics: Approaching a Complex World (Springer, New York) (2009).https://doi.org/10.1007/978-0-387-85359-8
18. C. Tsallis, R.S. Mendes, A.R. Plastino, Phys. A **261**, 534 (1998). https://doi.org/10.1016/S0378-4371(98)00437-3
19. T.S. Biro, G. Purcsel, K. Urmossy, Eur. Phys. J. A **40**, 325 (2009). https://doi.org/10.1140/epja/i2009-10806-6. arXiv:0812.2104
20. G. Wilk, Z. Wlodarczyk, Eur. Phys. J. A **40**, 299 (2009).https://doi.org/10.1140/epja/i2009-10803-9. arXiv:0810.2939
21. F.I.M. Pereira, R. Silva, J.S. Alcaniz, Phys. Lett. A **373**, 4214 (2009). https://doi.org/10.1016/j.physleta.2009.09.046. arXiv:0906.2422
22. J.M. Conroy, H.G. Miller, A.R. Plastino, Phys. Lett. A **374**, 4581 (2010). https://doi.org/10.1016/j.physleta.2010.09.038. arXiv:1006.3963
23. J. Cleymans, D. Worku, J. Phys. G **39**, 025006 (2012a). https://doi.org/10.1088/0954-3899/39/2/025006. arXiv:1110.5526
24. J. Cleymans, D. Worku, Eur. Phys. J. A **48**, 160 (2012b).https://doi.org/10.1140/epja/i2012-12160-0. arXiv:1203.4343
25. J.I. Kapusta, Int. J. Mod. Phys. E **30**, 2130006 (2021). https://doi.org/10.1142/S021830132130006X. arXiv:2106.06824
26. F.I.M. Pereira, R. SIlva, J.S. Alcaniz, Phys. Rev. C **76**, 015201 (2007).https://doi.org/10.1103/PhysRevC.76.015201. arXiv:0705.0300
27. J. Rozynek, G. Wilk, J. Phys. G **36**, 125108 (2009).https://doi.org/10.1088/0954-3899/36/12/125108. arXiv:0905.3408
28. J. Rożynek ,G. Wilk, Eur. Phys. J. A **52**, 13 (2016). [Erratum: Eur.Phys.J.A 52, 204 (2016)],https://doi.org/10.1140/epja/i2016-16013-6. arXiv:1510.08516
29. Y.-P. Zhao, Phys. Rev. D **101**, 096006 (2020). https://doi.org/10.1103/PhysRevD.101.096006. arXiv:2004.14556
30. G.S. Pradhan, D. Sahu, S. Deb, R. Sahoo, J. Phys. G **50**, 055104 (2023). https://doi.org/10.1088/1361-6471/acc478. arXiv:2106.14297
31. Y.-P. Zhao, C.-Y. Wang, S.-Y. Zuo, C.-M. Li, Chin. Phys. C **47**, 053103 (2023). https://doi.org/10.1088/1674-1137/acbf2a. arXiv:2302.12010
32. R.L.S. Farias, K.P. Gomes, G.I. Krein, M.B. Pinto, Phys. Rev. C **90**, 025203 (2014). https://doi.org/10.1103/PhysRevC.90.025203. arXiv:1404.3931
33. M. Ferreira, P. Costa, O. Lourenço, T. Frederico, C. Providência, Phys. Rev. D **89**, 116011 (2014). https://doi.org/10.1103/PhysRevD.89.116011. arXiv:1404.5577
34. A. Ayala, M. Loewe, R. Zamora, Phys. Rev. D **91**, 016002 (2015). https://doi.org/10.1103/PhysRevD.91.016002. arXiv:1406.7408
35. R.L.S. Farias, V.S. Timoteo, S.S. Avancini, M.B. Pinto, G. Krein, Eur. Phys. J. A **53**, 101 (2017). https://doi.org/10.1140/epja/i2017-12320-8. arXiv:1603.03847
36. A.N. Tawfik, A.M. Diab, N. Ezzelarab, A.G. Shalaby, Adv. High Energy Phys. **2016**, 1381479 (2016). https://doi.org/10.1155/2016/1381479. arXiv:1604.00043
37. A.N. Tawfik, A.M. Diab, M.T. Hussein, J. Phys. G **45**, 055008 (2018). https://doi.org/10.1088/1361-6471/aaba9e. arXiv:1604.08174
38. A.N. Tawfik, A.M. Diab, M.T. Hussein, J. Exp. Theor. Phys. **126**, 620 (2018). https://doi.org/10.1134/S1063776118050138. arXiv:1712.03264
39. A.N. Tawfik, A.M. Diab, Eur. Phys. J. A **57**, 200 (2021).https://doi.org/10.1140/epja/s10050-021-00501-z. arXiv:2106.04576
40. V. Miransky, I. Shovkovy, Phys. Rev. D **66**, 045006 (2002).https://doi.org/10.1103/PhysRevD.66.045006. arXiv:hep-ph/0205348
41. D.P. Menezes, M. BenghiPinto, S.S. Avancini, A. PerezMartinez, C. Providencia, Phys. Rev. C **79**, 035807 (2009). https://doi.org/10.1103/PhysRevC.79.035807. arXiv:0811.3361
42. J.K. Boomsma, D. Boer, Phys. Rev. D **81**, 074005 (2010). https://doi.org/10.1103/PhysRevD.81.074005. arXiv:0911.2164
43. B. Chatterjee, H. Mishra, A. Mishra, Phys. Rev. D **84**, 014016 (2011). https://doi.org/10.1103/PhysRevD.84.014016. arXiv:1101.0498
44. S.S. Avancini, D.P. Menezes, C. Providencia, Phys. Rev. C **83**, 065805 (2011). https://doi.org/10.1103/PhysRevC.83.065805
45. E. Ferrer, V. dela Incera, X. Wen, Phys. Rev. D **91**, 054006 (2015).https://doi.org/10.1103/PhysRevD.91.054006. arXiv:1407.3503
46. L. Yu, J. VanDoorsselaere, M. Huang, https://doi.org/10.1103/PhysRevD.91.074011 Phys. Rev. D **91**, 074011 (2015). arXiv:1411.7552
47. S. Mao, Phys. Lett. B **758**, 195 (2016). https://doi.org/10.1016/j.physletb.2016.05.018. arXiv:1602.06503
48. S.P. Klevansky, Rev. Mod. Phys. **64**, 649 (1992). https://doi.org/10.1103/RevModPhys.64.649
49. T. Hatsuda, T. Kunihiro, Phys. Rept. **247**, 221 (1994). https://doi.org/10.1016/0370-1573(94)90022-1. arXiv:hep-ph/9401310
50. M. Buballa, Phys. Rept. **407**, 205 (2005). https://doi.org/10.1016/j.physrep.2004.11.004. arXiv:hep-ph/0402234
51. P. Rehberg, S.P. Klevansky, J. Hufner, Phys. Rev. C **53**, 410 (1996). https://doi.org/10.1103/PhysRevC.53.410. arXiv:hep-ph/9506436
52. T.S. Biro, G. Purcsel, Phys. Rev. Lett. **95**, 162302 (2005).https://doi.org/10.1103/PhysRevLett.95.162302. arXiv:hep-ph/0503204
53. V.P. Gusynin, V.A. Miransky, I.A. Shovkovy, Nucl. Phys. B **462**, 249 (1996). https://doi.org/10.1016/0550-3213(96)00021-1. arXiv:hep-ph/9509320
54. V.P. Gusynin, I.A. Shovkovy, Phys. Rev. D **56**, 5251 (1997). https://doi.org/10.1103/PhysRevD.56.5251. arXiv:hep-ph/9704394
55. M. D'Elia, F. Manigrasso, F. Negro, F. Sanfilippo, Phys. Rev. D **98**, 054509 (2018). https://doi.org/10.1103/PhysRevD.98.054509. arXiv:1808.07008
56. G. Endrodi, JHEP **07**, 173 (2015). https://doi.org/10.1007/JHEP07(2015)173. arXiv:1504.08280
57. M. D'Elia, L. Maio, F. Sanfilippo, A. Stanzione, Phys. Rev. D **105**, 034511 (2022). https://doi.org/10.1103/PhysRevD.105.034511. arXiv:2111.11237

58. R. Hanel, S. Thurner, Europhys. Lett. **93**, 20006 (2011). https://doi.org/10.1209/0295-5075/93/20006
59. R. Hanel, S. Thurner, Europhys. Lett. **96**, 50003 (2011). https://doi.org/10.1209/0295-5075/96/50003
60. A. NasserTawfik, Eur. Phys. J. A **52**, 253 (2016). https://doi.org/10.1140/epja/i2016-16253-4. arXiv:1607.01264
61. A.N. Tawfik, H. Yassin, E.R. AboElyazeed, Chin. Phys. C **41**, 053107 (2017). https://doi.org/10.1088/1674-1137/41/5/053107. arXiv:1701.04697
62. A.N. Tawfik, H. Yassin, E.R. AboElyazeed, Indian J. Phys. **92**, 1325 (2018). https://doi.org/10.1007/s12648-018-1216-2. arXiv:1802.04912
63. A.N. Tawfik, Phys. Part. Nucl. Lett. **15**, 199 (2018). https://doi.org/10.1134/S1547477118030196. arXiv:1712.04807
64. S. Rath, S. Dash, Eur. Phys. J. C **83**, 867 (2023).https://doi.org/10.1140/epjc/s10052-023-12051-3. arXiv:2303.03071
65. S. Rath, S. Dash, Eur. Phys. J. A **60**, 29 (2024). https://doi.org/10.1140/epja/s10050-024-01252-3. arXiv:2307.12002
66. C.A. Islam, J. Dey, S. Ghosh, Phys. Rev. C **103**, 034904 (2021). https://doi.org/10.1103/PhysRevC.103.034904. arXiv:1901.09543
67. Z. Li, K. Xu, X. Wang, M. Huang, Eur. Phys. J. C **79**, 245 (2019). https://doi.org/10.1140/epjc/s10052-019-6703-x. arXiv:1801.09215